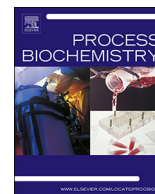




Contents lists available at ScienceDirect

Process Biochemistry

journal homepage: www.elsevier.com/locate/procbio

Characterization of a robust glucose 1-dehydrogenase, SyGDH, and its application in NADPH regeneration for the asymmetric reduction of haloketone by a carbonyl reductase in organic solvent/buffer system

Die Hu^{a,b,1}, Zheng Wen^{c,1}, Chuang Li^c, Bochun Hu^c, Ting Zhang^b, Jianfang Li^b, Minchen Wu^{a,*}

^a Wuxi School of Medicine, Jiangnan University, Wuxi, 214122, China

^b School of Food Science and Technology, Jiangnan University, Wuxi, 214122, China

^c School of Biotechnology, Jiangnan University, Wuxi, 214122, China

ARTICLE INFO

Keywords:

Glucose 1-dehydrogenase
Coenzyme regeneration
Carbonyl reductase
Organic solvent/buffer
System
Haloketone
Enantiopure halohydrin

ABSTRACT

To realize coenzyme regeneration in the reduction of haloketones, a codon-optimized gene *Sygdh* encoding glucose 1-dehydrogenase (SyGDH) was synthesized based on the putative GDH gene sequence (Ta0897) in *Thermoplasma acidophilum* genomic DNA, and expressed in *E. coli* BL21(DE3). Recombinant SyGDH was purified to homogeneity by affinity chromatography with the specific activity of 86.3 U/mg protein towards D-glucose at the optimum pH and temperature of 7.5 and 40 °C. It was highly stable in a pH range of 4.5–8.0 and at 60 °C or below, and resistant to various organic solvents. The K_m and catalytic efficiency (k_{cat}/K_m) of SyGDH towards NADP⁺ were 0.67 mM and 104.0 mM⁻¹ s⁻¹, respectively, while those towards NAD⁺ were 157.9 mM and 0.64 mM⁻¹ s⁻¹, suggesting that it preferred NADP⁺ as coenzyme to NAD⁺. Additionally, using whole cells of *E. coli*/Sygdh-Sys1, coexpressing SyGDH and carbonyl reductase (SyS1), as the biocatalyst, the asymmetric reduction of 60 mM *m*-chlorophenacyl chloride coupled with the regeneration of NADPH *in situ* was conducted in DMSO/phosphate buffer (2:8, v/v) system, producing (*R*)-2-chloro-1-(3-chlorophenyl)ethanol with over 99.9% ee_p and 99.2% yield. Similarly, the reduction of 40 mM α -bromoacetophenone in *n*-hexane/buffer (6:4, v/v) biphasic system produced (*S*)-2-bromo-1-phenylethanol with over 99.9% ee_p and 98.3% yield.

1. Introduction

Various NAD(P)H-dependent dehydrogenases have been broadly applied in producing the highly value-added and versatile enantiopure building blocks, such as halohydrins, aryl alcohols and alcohols, for the synthesis of pharmaceuticals, agrochemicals and fine chemicals [1–3]. For example, (*R*)-2-chloro-1-(3-chlorophenyl)ethanol (CCE) and (*S*)-2-bromo-1-phenylethanol (BPE) are crucial drug intermediates used for the synthesis of adrenergic receptor agonists, bronchodilators, antidepressants, and HIV-1 protease inhibitors [4,5]. To tackle the issue of the overconsumption of expensive coenzymes, such as NAD(P)H, in reduction reactions, the regeneration of coenzymes *in situ* by dehydrogenases has been considered as an effective strategy [6]. NAD(P)⁺-dependent glucose 1-dehydrogenases (GDHs, EC 1.1.1.47) can catalyze the oxidation of D-glucose into β -D-glucono-1,5-lactone coupled with the reduction of NAD(P)⁺ into NAD(P)H. In contrast with other dehydrogenases, such as alcohol dehydrogenases (ADHs) [7], formate

dehydrogenases (FDHs) [8] and lactate dehydrogenases (LDHs) [9], GDHs can utilize either NAD⁺ or NADP⁺ as coenzyme and the low-cost D-glucose as substrate, thereby being a component of a well-established method for coenzyme regeneration in biocatalysis [10].

A variety of GDHs, belonging to the short-chain dehydrogenase/reductase (SDR) family, extensively exist in *Bacillus* species, such as GDHs from *B. subtilis* (*BsGDH*) [11], *B. megaterium* (*BmGDH*) [12], *B. cereus* (*BcGDH*) [13] and *B. amyloliquefaciens* SB5 (*BaGDH*) [14] (Table S1). Among them, *BsGDH* and *BmGDH* are the most commonly used enzymes for the coenzyme regeneration, which have high specificity toward D-glucose but low thermostability and organic solvent tolerance [15,16]. Compared with aqueous phase biocatalysis, the organic/aqueous biphasic biocatalysis possesses some distinctive advantages, such as the high solubility and stability of substrates and products, avoidance of side reactions and enhancement of product enantiomeric purity [17]. In general, however, due to the organic solvents induce enzymes to easily inactivation, organic solvent-tolerant GDHs are urgently required

* Corresponding author.

E-mail address: biowmc@126.com (M. Wu).

¹ These authors contributed equally to this paper.

<https://doi.org/10.1016/j.procbio.2019.09.037>

Received 8 July 2019; Received in revised form 27 September 2019; Accepted 29 September 2019

1359-5113/© 2019 Elsevier Ltd. All rights reserved.

for the regeneration of NAD(P)H in the organic/aqueous biphasic system.

The whole genome of *T. acidophilum* DSM 1728 has been sequenced, in which three putative SDR family GDH genes (GenBank accession nos. AL445065: Ta0747 and Ta0754; AL445063: Ta0191) and one putative medium-chain dehydrogenase/reductase (MDR) family GDH gene (AL445065: Ta0897) have been identified [18]. Both Ta0754 and Ta0191 genes were expressed in *E. coli*, respectively, while other two genes have not been heterogeneously expressed. The expressed Ta0754 and Ta0191 GDHs exhibited NAD⁺ and NADP⁺ dependences, respectively, but both low specific activities towards D-glucose (3.5 and 3.1 U/mg) [19,20]. To date, several studies have been performed on the characterization of purified *T. acidophilum* GDH (*TaGDH*) [21], the expression of *TaGDH* gene (GenBank: X59788, encoding 353 residues) in *E. coli* [22], the determination of *TaGDH* crystal structure [23], and the application of *TaGDH* in coenzyme regeneration [24]. However, the amino acid sequence of *TaGDH* in the C-terminus is significantly different from that deduced from the putative MDR family GDH gene (Ta0897, encoding 361 residues).

In our previous studies, a SyGDH-encoding gene *Sygdh* was synthesized based on the putative GDH gene (Ta0897) in *T. acidophilum* genome. Meanwhile, the SyS1-encoding gene, *Sys1* was synthesized with optimized codons based on the carbonyl reductase gene from *Candida magnoliae* (GenBank: AB036927) [25]. In this work, both *Sygdh* and *Sys1* were separately expressed and coexpressed in *E. coli* BL21(DE3). The pH and temperature properties, substrate and coenzyme specificity, and organic solvent tolerance of purified SyGDH were characterized. Additionally, the whole cells of *E. coli/Sygdh-Sys1* coexpressing SyGDH and SyS1 were applied to the asymmetric reduction of *m*-chlorophenacyl chloride (*m*-CPC) and α -bromoacetophenone (α -BAP) coupled with NADPH regeneration in situ in an organic solvent/phosphate buffer system. Our studies not only completed the catalytic properties of the robust SyGDH, but also provided a reference for the application of GDHs in the coenzyme regeneration.

2. Materials and methods

2.1. Strains, plasmids and chemicals

E. coli BL21(DE3) and single and double promoter plasmids (pET-28a(+)) and pETDuet-1 (Novagen, Madison, WI) were used for gene expression. *E. coli* transformants, *E. coli/Sygdh* and *E. coli/Sys1* (separately expressing SyGDH and SyS1) and *E. coli/Sygdh-Sys1* (coexpressing two enzymes), were constructed and preserved in our lab [25]. *E. coli* BL21(DE3) transformed with pET-28a(+) and pETDuet-1, designated as *E. coli/pET-28a* and *E. coli/pETDuet*, were used as the negative control. Reduced and oxidized nicotinamide adenine dinucleotide (phosphate), coenzymes NAD(P)H and NAD(P)⁺, were purchased from YuanYe Biotechnology (Shanghai, China). Both *m*-CPC and α -BAP as well as the corresponding racemic 2-chloro-1-(3-chlorophenyl)ethanol (*rac*-CCE) and *rac*-BPE were purchased from Sun Chemical Technology (Shanghai, China).

2.2. Expression and purification

A single colony of *E. coli* transformant was inoculated into 2 mL LB medium supplemented with 100 μ g/mL kanamycin for *E. coli/Sygdh* or with 100 μ g/mL ampicillin for *E. coli/Sys1* and */Sygdh-Sys1*, and cultured at 37 °C overnight as the seed culture. Then, 30 mL fresh LB medium was inoculated with 2% (v/v) seed culture, and cultured until the optical density at 600 nm (OD₆₀₀) reached 0.6–0.8. The expression of SyGDH and SyS1 and coexpression of both SyGDH and SyS1 were induced, respectively, by addition of 0.6 mM IPTG at 25 °C for 10 h. The induced *E. coli* cells were harvested by centrifugation, and resuspended in 50 mM K₂HPO₄-KH₂PO₄ buffer (pH 7.0) to 100 mg wet cells/mL unless stated otherwise.

The recombinantly expressed SyGDH and SyS1 harboring a 6 \times His tag at its N-terminus were purified by affinity chromatography using a nickel-nitrilotriacetic acid (Ni-NTA) column (Tiandz, Beijing, China). The purity and the concentration of SyGDH and SyS1 were analyzed by SDS-PAGE and the BCA-200 protein assay kit (TaKaRa, Dalian, China), respectively.

2.3. Activity assays of SyGDH and SyS1

The SyGDH activity was assayed at 40 °C in a 96-well plate, in which each well contained 50 mM glucose and 2 mM NADP⁺ in 50 mM phosphate buffer (pH 7.5). Then, the reaction, in a final volume of 220 μ L, was initiated by the addition of a certain amount of purified SyGDH, and continuously monitored for an increase in OD₃₄₀ using a Synergy™ H4 multi-mode microplate reader (BioTek, Winooski, VT). Similarly, for the SyS1 activity assay, each well contained 20 mM α -BAP and 2 mM NADPH in the same buffer and a certain amount of purified SyS1 in a final volume of 220 μ L, and the decrease in OD₃₄₀ was measured [25]. One activity unit (U) was defined as the amount of enzyme catalyzing the reduction of 1 μ mol NADP⁺ per minute (for SyGDH) or the oxidation of 1 μ mol NADPH per minute (for SyS1) under the given assay conditions.

2.4. pH and temperature properties of the purified SyGDH

The pH optimum of purified SyGDH was determined under the standard assay conditions, except for 50 mM different buffers (Na₂HPO₄-citric acid: pH 4.0–7.0 and Tris-HCl: pH 7.5–9.0) were used. To evaluate the pH stability, aliquots of SyGDH solution were incubated in the absence of substrate, in a pH range of 4.0–9.0 and at 40 °C for 1 h. Additionally, aliquots of purified SyGDH were incubated at pH values of 4.5, 5.5, 6.5 and 7.5 at 25 °C, respectively, for 1, 2, 4, 6, 8, 10, and 12 h. Then, the residual activity was measured under the standard assay conditions.

The temperature optimum of purified SyGDH was measured at the optimum pH over temperatures ranging from 10 to 70 °C. To estimate the thermostability, aliquots of purified SyGDH were incubated at 10–70 °C for 1 h, respectively. Additionally, the aliquots of purified SyGDH were incubated at 40 °C, 50 °C and 60 °C at a pH of 7.5, respectively, for 1, 2, 4, 6, 8, 10, and 12 h. Then, the residual activity was measured under the standard assay conditions. The pH stability and thermostability were defined as the temperature and pH range, respectively, in which the residual activity of SyGDH was over 80% of its original activity. The half-life was defined as the time, at which the residual activity of SyGDH was 50% of its original activity.

2.5. Effects of metal ions and EDTA on the activity of SyGDH

To estimate the effects of metal ions and EDTA on the activity of SyGDH, aliquots of purified SyGDH without preprocessing by EDTA were incubated ZnCl₂, FeCl₂, CoCl₂, MgSO₄, LiCl, SnCl₂, FeCl₃, NaCl, AlCl₃, BaCl₂, CaCl₂, CuSO₄, or EDTA solution (50 mM, dissolved in water) at a final concentration of 2 mM, respectively, in 20 mM phosphate buffer (pH 7.5) at 40 °C for 1 h. Then, the residual enzyme activity was measured under the standard assay conditions. Additionally, the activity of SyGDH incubated in the 2 mM EDTA was measured by addition of extra 5 mM ZnCl₂. Enzyme without adding any additive was used as the control.

2.6. Substrate and coenzyme specificities of SyGDH

The substrate specificity of SyGDH was investigated by measuring its specific activities (U/mg protein) towards 50 mM different mono- and di-saccharides (such as D-glucose, D-galactose, D-xylose, D-mannose, D-maltose, glucose 6-phosphate and sucrose) under the standard assay conditions. The oxidation rate of D-glucose (μ mol/min/mg

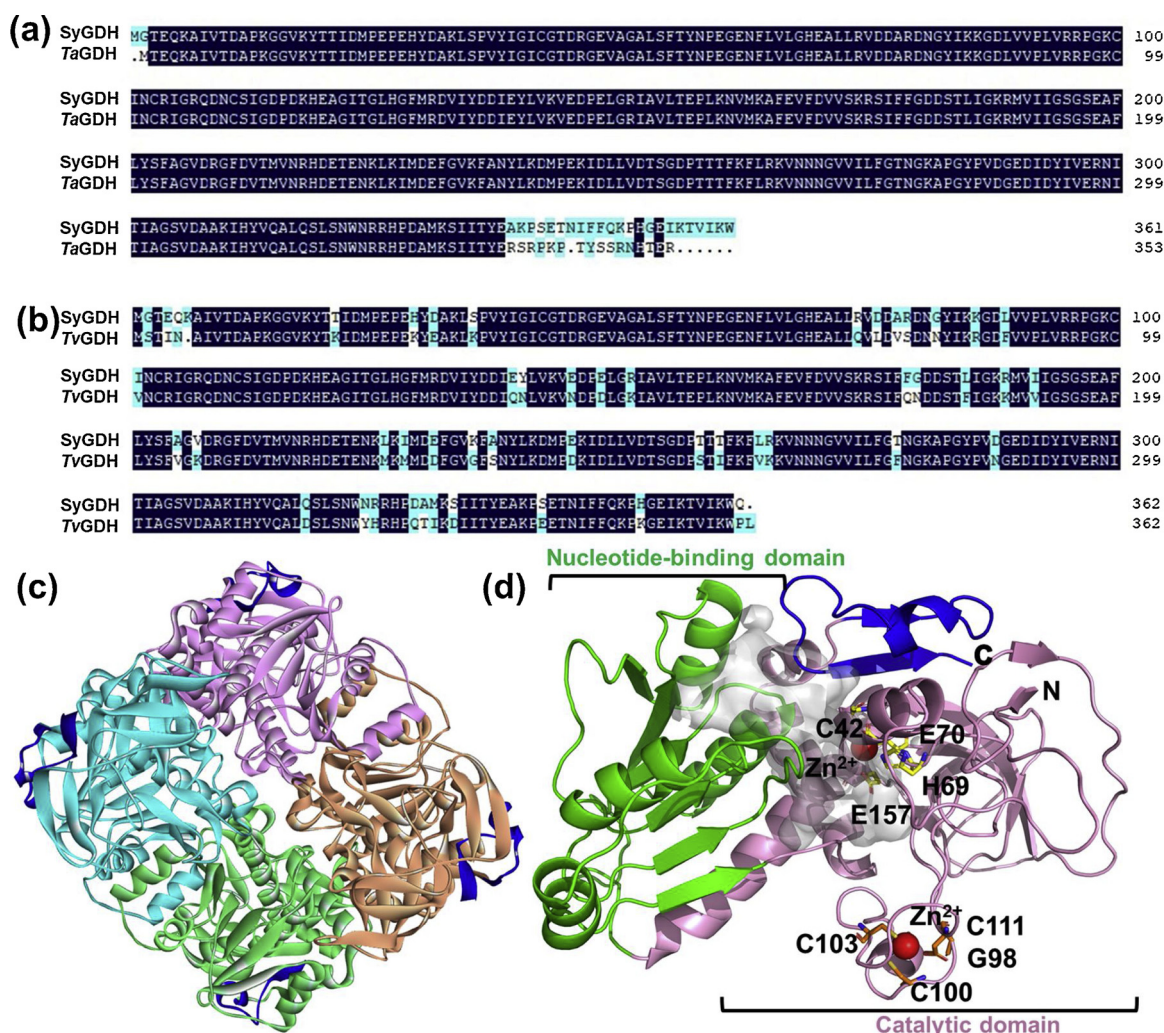


Fig. 1. The primary and 3-D structures of SyGDH. (a) The primary structural alignment of SyGDH and TgGDH. (b) The primary structural alignment of SyGDH and TvGDH. (c) The homology tetramer model of SyGDH was constructed based on the X-ray structure of TvGDH (PDB ID: 3WIC) using SWISS-MODEL software. The C-terminus of SyGDH are shown in blue cartoon. (d) The modeled 3-D structure of SyGDH. The catalytic domain, nucleotide-binding domain and C-terminus of SyGDH are shown in pink, green and blue cartoons, respectively, two Zn^{2+} in red balls, residues C42, E70, H69 and E157 in yellow sticks, and residues C98, C100, C103 and C111 in orange sticks (For interpretation of the references to colour in this figure legend, the reader is referred to the web version of this article).

protein) by purified SyGDH was measured under its activity assay conditions, except for D-glucose concentrations ranging from 5.0 to 50 mM using 2.0 mM $NADP^+$ as coenzyme. Analogously, the reduction rate of $NADP^+$ and NAD^+ by SyGDH were measured under its activity assay conditions, except for coenzyme $NADP^+$ concentrations from 1.0 to 2 mM or NAD^+ concentrations from 10 to 100 mM. Both K_m and V_{max} values towards D-glucose, $NADP^+$ and NAD^+ were calculated by nonlinear regression analysis, respectively. The specific activity versus the concentration of D-glucose, $NADP^+$ and NAD^+ was plotted with the Michaelis-Menten equation. The turnover number (k_{cat}) of SyGDH was deduced from its V_{max} and apparent molecular weight, while its catalytic efficiency (k_{cat}/K_m) was defined as the ratio of k_{cat} to K_m .

2.7. Effect of organic solvents on the stability of SyGDH

Aliquots of purified SyGDH were incubated in 1 mL different organic solvent/buffer (1:1, v/v) solutions at 25 °C and 220 rpm for 1, 2, 4, 6, 8, 10, and 12 h, where the organic solvents included water-miscible solvents (methanol, ethanol, isopropanol, *N,N*-dimethylformamide (DMF), dimethyl sulfoxide (DMSO) and isobutanol) and water-immiscible solvents (*n*-pentanol, *n*-octanol, *n*-hexane, *n*-octane, cyclohexane, isooctane, *n*-heptane, methyl tertiary butyl ether (MTBE), ethyl

acetate and *n*-butyl acetate). Then, 50 μ L solution was withdrawn from the mixed water-miscible solvent/buffer solutions, while aqueous solution from the water-immiscible solvent/buffer solutions, respectively, to measure the residual activity under the standard assay conditions.

2.8. Asymmetric reduction of *m*-CPC by *E. coli*/Sygdh-Sys1 in the DMSO/buffer system

The asymmetric reduction of *m*-CCE was carried out in 5 mL DMSO/buffer system containing 60 mM *m*-CPC, 0.2 mM $NADP^+$, 80 mM D-glucose, 20% (v/v) DMSO as cosolvent and 70 mg/mL *E. coli*/Sygdh-Sys1 wet cells at 40 °C and 220 rpm. Aliquots of 100 μ L sample were withdrawn periodically, extracted by ethyl acetate and analyzed to monitor the reaction process by chiral gas chromatography (GC) using a GC-2010 apparatus (Shimadzu, Tokyo, Japan) equipped with a chiral CP-Chirasil-DEX CB column (Agilent, Santa Clara, CA; 30 m \times 0.25 mm \times 0.25 μ m) and a flame ionization detector. The injector and detector temperatures were 220 °C, the column temperature was programmed from 80 to 150 °C at a rate of 5 °C/min and maintained at 150 °C for 5 min. The *ee* and molar yield of (*R*)-CCE were calculated with the following equations: $ee = (R_p - S_p) / (R_p + S_p) \times 100\%$ and $yield = (R_p + S_p) / S_0 \times 100\%$, where R_p and S_p are the concentrations

of (R)–CCE and (S)–CCE, while S_0 is the initial concentration of *m*-CPC.

2.9. Asymmetric reduction of α -BAP in the *n*-hexane/buffer biphasic system

The asymmetric reduction of α -BAP was carried out in 5 mL *n*-hexane/buffer biphasic system containing 40 mM α -BAP, 0.2 mM NADP^+ , 80 mM D-glucose, 60% (v/v) *n*-hexane as cosolvent and 70 mg/mL *E. coli/Sygdh-Sys1* wet cells at 40 °C and 220 rpm. Aliquots of 100 μL sample were withdrawn periodically, extracted by ethyl acetate and analyzed to monitor the reaction process by chiral GC. The chiral GC conditions are the same as described above, except the column temperature was programmed from 100 to 200 °C at a rate of 10 °C/min. The *ee* and molar yield of (S)-BPE were calculated with the following equations: $ee = (S_p - R_p) / (S_p + R_p) \times 100\%$ and $yield = (R_p + S_p) / S_0 \times 100\%$, where R_p and S_p are the concentrations of (S)-BPE and (R)-BPE, and while S_0 is the initial concentration of α -BAP, respectively. The total turnover number (TTN) of NADP^+ was defined as the total amount of the formed (R)–CCE or (S)-BPE consuming 1 μmol NADP^+ in the biocatalytic system.

3. Results and discussion

3.1. Analysis the primary and three-dimensional (3-D) structures of SyGDH

The codon-optimized *Sygdh* gene (containing the *Nco* I site at the 5'-end) is 1089 bp in length and encodes 362 residues (GenBank: [AH117928](#)). The primary structure of SyGDH exhibited less than 16.2% identity with those of Ta0754, Ta0754 and Ta0191 [19], and low similarities to known GDHs from *Bacillus* species [26]. A BLAST search indicated that SyGDH showed less than 60% sequence identity with other GDHs, except for TaGDH (98.5%) [23] and TvGDH from *T. volcanium* (86.1%) [27] (Table S1). Interestingly, the primary structure of SyGDH was the same as that of TaGDH except for the significant difference in the C-terminus (Fig. 1a), which was highly similar to that of TvGDH (Fig. 1b). A homology tetramer model of SyGDH was obtained based on the X-ray structure of TvGDH (PDB ID: 3WIC, 86.1% identity) [27] using SWISS-MODEL software (<https://swissmodel.expasy.org/>) [28] (Fig. 1c). As shown in Fig. 1d, each monomer consists of two domains: a catalytic domain (residues 1–185, 298–363) and a nucleotide-binding domain (residues 185–298). A putative substrate-binding pocket of SyGDH located in the middle of two domains. The C-terminus of SyGDH (blue) contains an α -helix and two parallel β -strands, which was different from the structure of TaGDH, whose C-terminus is a long disordered loop [23]. By superimposing the 3-D structure of TaGDH onto that of TvGDH, it was presumed that one catalytic Zn^{2+} -binding site of SyGDH consisted of residues C42, H69, E70 and E157, and that the other site consists of residues G98, C100, C102 and C111.

3.2. Enzymatic properties of the purified SyGDH

SyGDH was purified to homogeneity by a Ni-NTA column with apparent molecular weight of 41.0 kDa, which was close to the theoretical molecular weight of 41,260 Da (Fig. 2). As shown in Fig. 3a and c, the purified SyGDH showed the highest activity of 86.3 U/mg at a pH of 7.5 and 40 °C, which was different from the activity of TaGDH (458 U/mg at optimum pH 6.5 and 55 °C) [22], indicating that the C-terminus of SyGDH located on surface of the tetramer structure (Fig. 1c) and near the active center (Fig. 1d) plays a significant influence on the activity and pH and temperature properties. In addition, it exhibited high specific activity in a pH range of 6.0–7.5 and at 20–60 °C, as well as high stability (retaining more than 80% activity for 1 h) in a pH range of 4.5–8.0 and at 60 °C or below. The half-lives of SyGDH at pH values of 4.5, 5.5, 6.5 and 7.5 were 8, 9 and 10 h (Fig. 3b), and at 40, 50 and 60 °C were 12, 8 and 6 h, respectively (Fig. 3d). Comparatively, the optimum temperature (40 °C) of SyGDH was lower than those of other

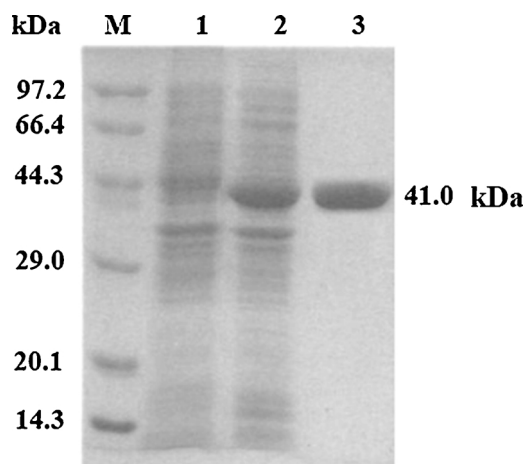


Fig. 2. SDS-PAGE analysis of the expressed SyGDH. Lane 1, the cell lysate of uninduced *E. coli/Sygdh*; Lane 2, the cell lysate of induced *E. coli/Sygdh*; Lane 3, the purified SyGDH.

GDHs from thermoacidophilic archaea, such as TvGDH (70 °C) [27] TgGDH (85 °C) [29], and TtGDH (70 °C) [30], which showed low activity at room temperature. Moreover, the thermostability of SyGDH was significantly higher than those of GDHs from *Bacillus* species, such as BsGDH (a half-life of 20 min at 25 °C) [15], BmGDH (inactivation at 60 °C for 20 min) [12] and ByGDH (inactivation at 45 °C for 1 h) [31] (Table S2). The acidophilia and acid resistance of SyGDH were remarkably superior to those of GDHs from *Bacillus* species (Table S2), which was advantageous as the pH value decreased with the autohydrolysis of β -D-glucono-1,5-lactone forming D-gluconic acid in the aqueous reaction system. Therefore, the mild optimum temperature, high thermostability and wide pH tolerance make SyGDH an attractive participant for coenzyme regeneration in biocatalysis. Investigation of the effects of metal ions and EDTA on the activity of SyGDH showed that its activity was inhibited obviously by Cu^{2+} and EDTA, while promoted by Zn^{2+} (Fig. 4). In addition, the SyGDH activity with pre-processing by 2 mM EDTA was recovered to the initial activity by addition of 5 mM Zn^{2+} , demonstrating Zn^{2+} played an important role on SyGDH activity.

The specific activities of the purified SyGDH towards D-glucose and D-galactose were measured to be 86.3 and 78.3 U/mg, respectively, using 2 mM NADP^+ as coenzyme, respectively, but SyGDH showed no activity towards D-xylose, D-mannose, D-maltose, glucose 6-phosphate and sucrose. Although SyGDH exhibited both NADP^+ and NAD^+ dependences, its specific activity of SyGDH towards D-glucose was only 8.5 U/mg using 2 mM NAD^+ as coenzyme. The K_m values of SyGDH towards D-glucose, NADP^+ and NAD^+ were 7.48, 0.67 and 157.9 mM, which were close to those of the purified TaGDH (10.3, 0.11 and > 30 mM) [21]. The catalytic efficiency (k_{cat}/K_m) of SyGDH towards NADP^+ ($104.0 \text{ s}^{-1} \text{ mM}^{-1}$) was obviously higher than that towards NAD^+ ($0.64 \text{ s}^{-1} \text{ mM}^{-1}$), suggesting that it preferred NADP^+ as coenzyme to NAD^+ (Table 1, Fig. S2). The narrow substrate specificity and NADP^+ preference towards D-glucose of SyGDH were similar to those exhibited by TaGDH [21], TvGDH [27] and PtGDH [32], but different from those displayed by NAD^+ -preference SsGDH2 [33] and TgGDH [29] with strict specificity towards D-glucose, as well as SsGDH1 (NAD^+ preference) [33] and HmGDH (NADP^+ preference) [34] with broad substrate specificity. Compared with BsGDH [15], BmGDH [12] and BtGDH [35], SyGDH had approximate k_m towards NADP^+ but higher K_m towards NAD^+ , indicating that it is suitable for NADPH rather than NADH regeneration (Table S2).

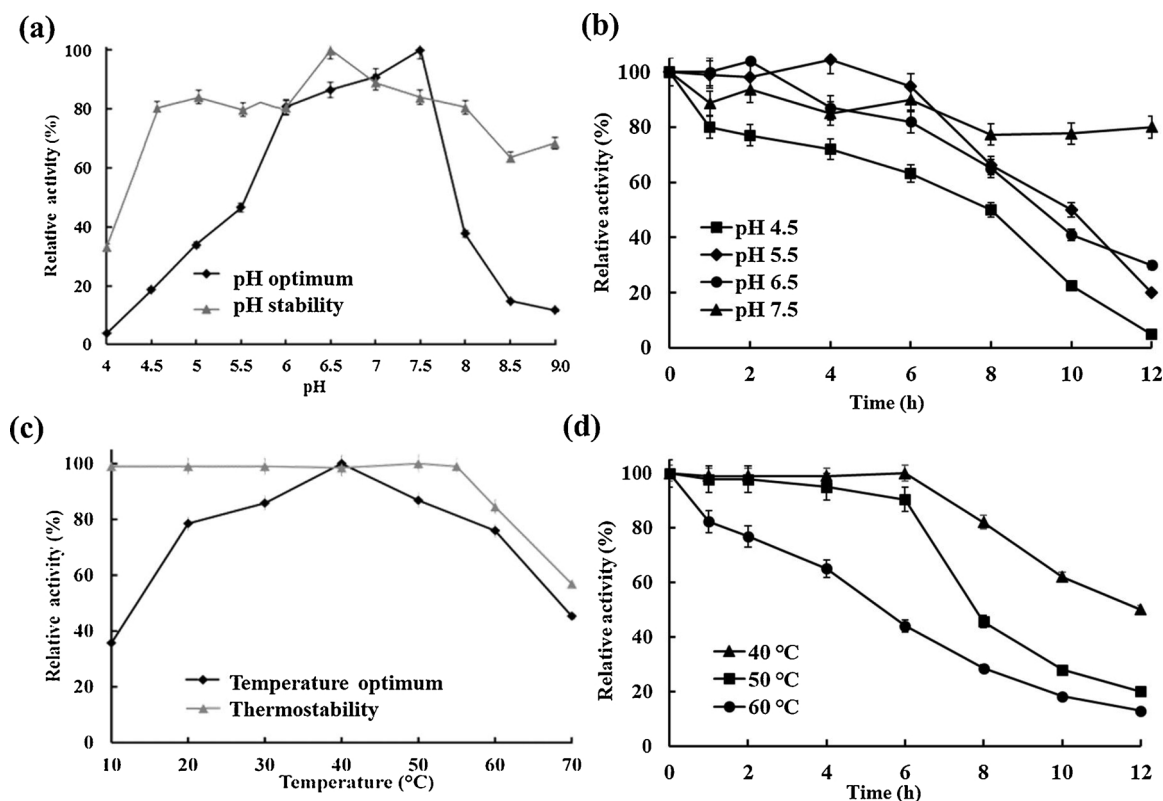


Fig. 3. Effects of the pH (a and b) and temperature (c and d) on the activity and stability of purified SyGDH.

3.3. Organic solvent tolerances of SyGDH

To overcome the drawbacks of the low solubility and poor stability of organic substrates and/or products in the conventional aqueous phase, the addition of organic solvents to the biocatalytic systems is a promising approach to improve the productivity [17]. Therefore, the organic solvent tolerance of biocatalysts should be considered, when the organic solvent/buffer mixture was used as the reaction system. As shown in Fig. 5, after incubation in different organic solvent/buffer (1:1, v/v) systems at 40 °C and 220 rpm for 12 h, SyGDH was considerably stable in the majority of selected solvents, retaining over 90%

Table 1

The kinetic parameters of the purified SyGDH towards D-glucose, NADP⁺ and NAD⁺.

Substrate	K_m (mM)	V_{max} (U/mg)	k_{cat} (s ⁻¹)	k_{cat}/K_m (s ⁻¹ ·mM ⁻¹)
D-glucose	7.48 ± 0.37	95.0 ± 2.1	64.9	8.67
NADP ⁺	0.67 ± 0.13	102.0 ± 2.1	69.7	104.0
NAD ⁺	157.9 ± 4.7	149.2 ± 3.4	101.9	0.64

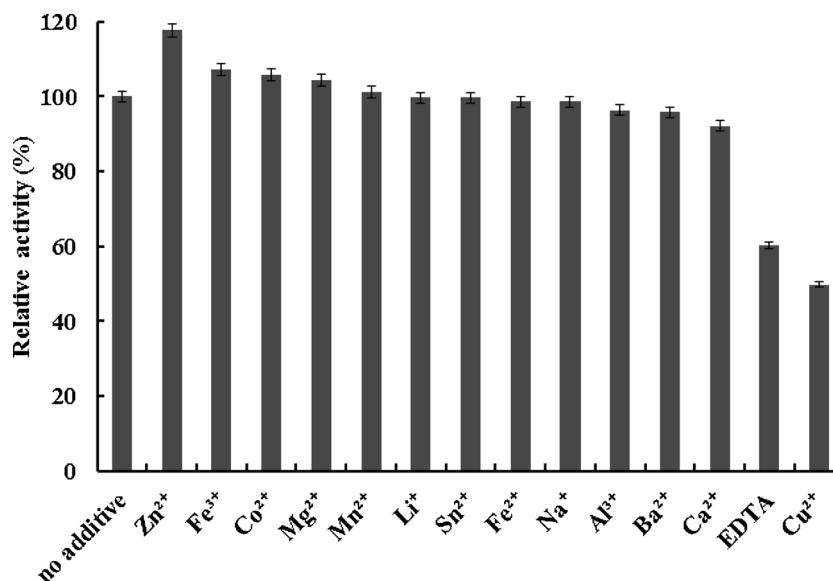


Fig. 4. Effects of metal ions and EDTA on the activity of purified SyGDH.

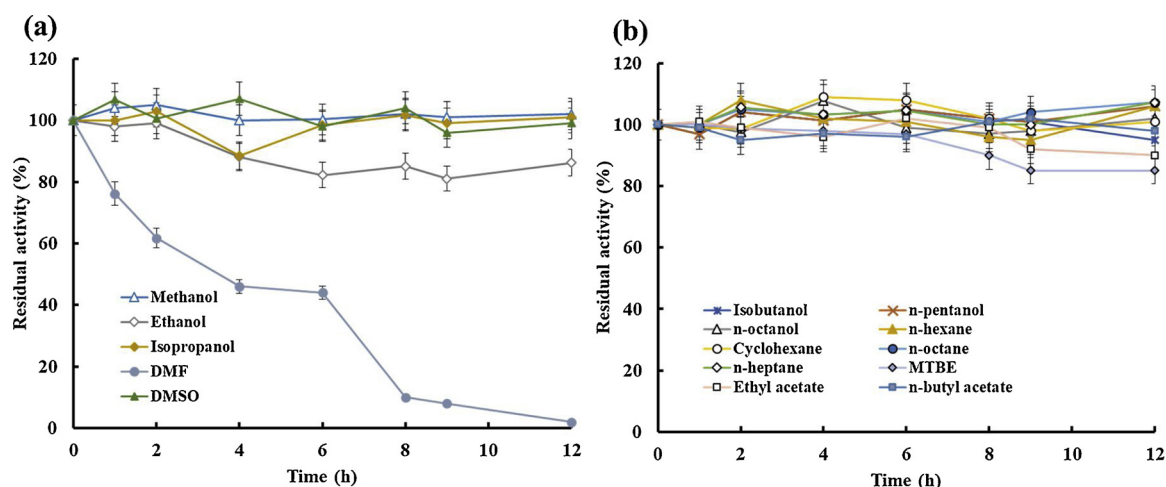


Fig. 5. Effects of water-miscible (a) and water-immiscible solvents (b) on the stability of purified SyGDH.

activity, except for DMF with a half-life of 3 h. Compared with *LsGDH* [36], *BcGDH* [13] and *BaGDH* [14], which were nearly completely inactivated in 50% acetone, ethanol, *n*-butanol and *n*-hexanol for 1 h, SyGDH displayed a higher organic solvent tolerance, thus extending its applicability in biocatalysis.

3.4. The production of (*R*)-CCE from *m*-CPC by *E. coli*/*Sygdh-Sys1* in the DMSO/buffer system

In our previous study, *E. coli*/*Sygdh-Sys1* was applied to the asymmetric reduction of *m*-CPC at a concentration of 30 mM in phosphate buffer system (10% methanol as cosolvent), producing (*R*)-CCE in high *ee* and yield [25]. However, the low solubility of *m*-CPC in aqueous solution was an important factor limiting the productivity of (*R*)-CCE. In this work, DMSO was selected as cosolvent to construct a DMSO/buffer system, in which *m*-CPC had high solubility and both SyGDH and

SyS1 were stable (Fig. 3 and Fig. S1). As shown in Fig. 6a, 60 mM *m*-CPC was catalyzed by *E. coli*/*Sygdh-Sys1* in different DMSO/buffer systems. After incubation at 40 °C and 220 rpm for 12 h, the yield of (*R*)-CCE was only 5.1% without addition of any cosolvent, but over 99.9% with addition of 20% (*v/v*) DMSO. The biocatalytic process for the asymmetric reduction of 60 mM *m*-CPC by *E. coli*/*Sygdh-Sys1* in the DMSO/buffer (2:8; *v/v*) system was monitored by chiral GC. After reaction for 3 h, (*R*)-CCE was obtained with over 99.9% *ee* and 99.2% yield (Fig. 6b, c and d). The total turnover number (TTN) of NADP⁺ and space time yield (STY) of (*R*)-CCE were 300 mol/mol and 3.8 g/L/h, respectively, which were 2-fold higher than those performed in the phosphate buffer system [25]. Moreover, the reduction of *m*-CPC catalyzed by *E. coli*/*Sygdh-Sys1* displayed lower cell dosage (70 mg/mL), higher productivity (3.8 g/L/h) and shorter reaction time (3 h) than those catalyzed by whole cells of *Saccharomyces cerevisiae* (100 mg/mL, 3.8 g/L/h, 48 h) [37] and *Candida ontarioensis* (200 mg/mL, 0.59 g/L/h,

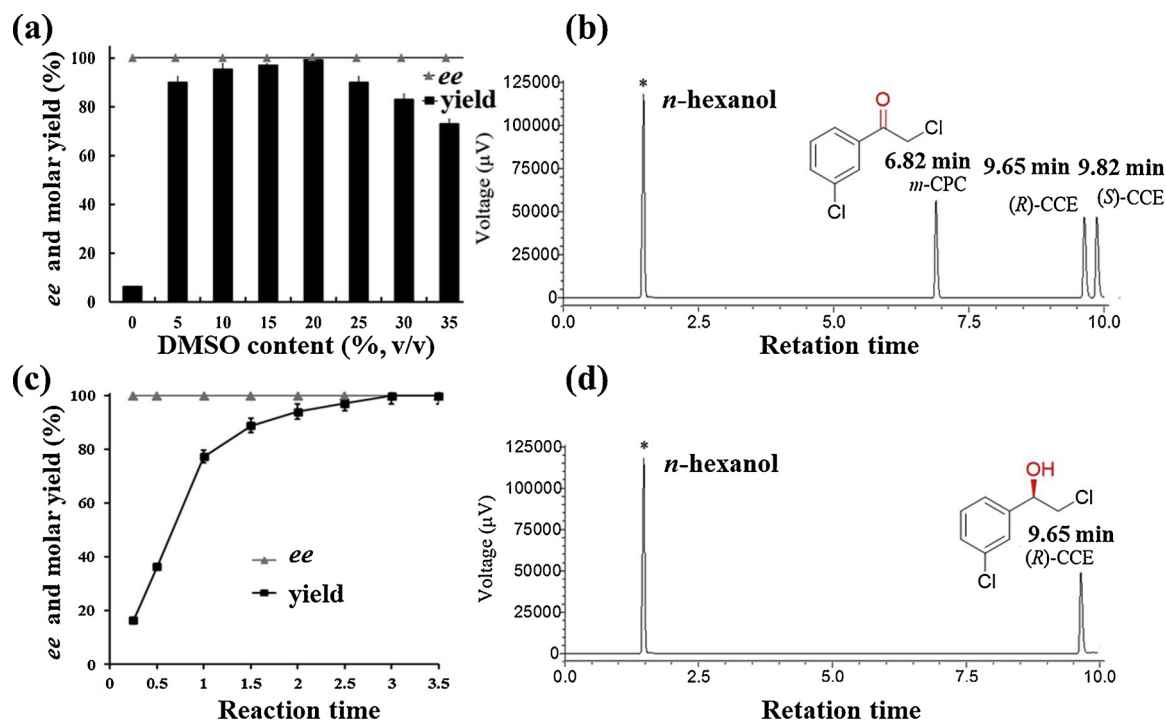


Fig. 6. Asymmetric reduction of *m*-CCE by *E. coli*/*Sygdh-Sys1* in the DMSO/buffer system. (a) Optimization of the amount of DMSO added. (b) The retention times of the standard *m*-CPC, (*R*)- and (*S*)-CCE analyzed by chiral GC. (c) The biocatalytic process for the asymmetric reduction of *m*-CCE by *E. coli*/*Sygdh-Sys1* in the DMSO/buffer (2:8, *v/v*) system. (d) The retention time of the reaction sample analyzed by chiral GC.

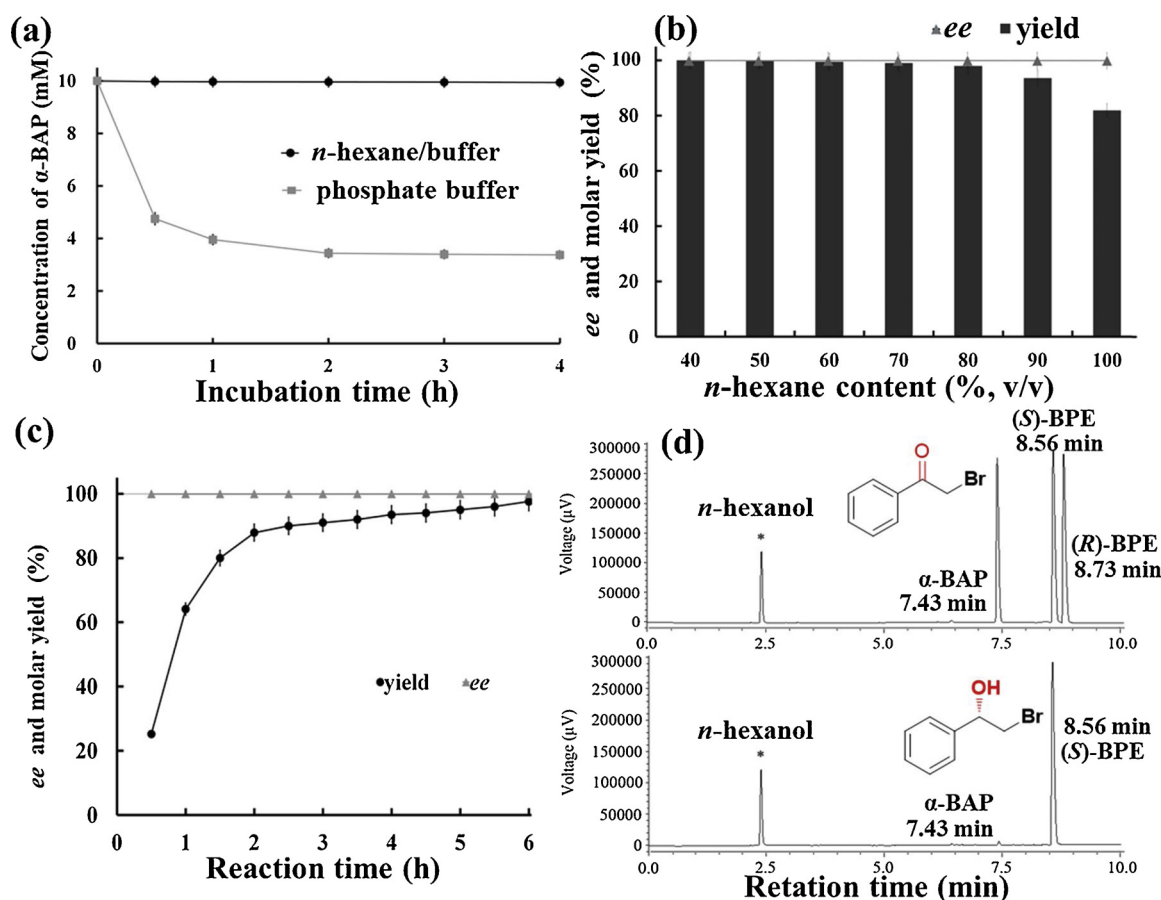


Fig. 7. Asymmetric reduction of α -BAP by *E. coli/Sygdh-Sys1* in the *n*-hexane/buffer system. (a) The stability of α -BAP incubated in phosphate buffer or *n*-hexane/buffer (1:1, v/v) system at 40 °C and 220 rpm for 4 h. (b) Optimization of the amount of *n*-hexane added. (c) The biocatalytic process for the asymmetric reduction of α -BAP by *E. coli/Sygdh-Sys1* in an *n*-hexane/buffer (6:4, v/v) system. (d) The retention time of the standard *m*- α -BAP, (R)- and (S)-BPE, and the reaction sample analyzed by chiral GC.

24 h) [38].

3.5. The production of (S)-BPE from α -BAP by *E. coli/Sygdh-Sys1* in the *n*-hexane/buffer biphasic system

Many ketones were reduced asymmetrically to chiral alcohols by different carbonyl reductases [39–41], but there were few reports on the enzymatic reduction of α -BAP, mainly due to its instability in aqueous solution due to the spontaneous debromination [5]. As shown in Fig. 7a, the instability of α -BAP was confirmed by the incubation of 10 mM α -BAP in phosphate buffer system, where the concentration of α -BAP decreased rapidly to 3.2 mM within 2 h. In contrast, α -BAP was stable in the *n*-hexane/buffer (1:1, v/v) system, in which no decomposition of α -BAP was observed after incubation for 4 h. After 40 mM α -BAP was catalyzed by *E. coli/Sygdh-Sys1* in different *n*-hexane/buffer biphasic systems at 40 °C and 220 rpm for 12 h, (S)-BPE was obtained with over 98% yield in the biphasic reaction systems with the addition of 40–60% (v/v) *n*-hexane in reaction system (Fig. 7b). The biocatalytic process for the asymmetric reduction of 40 mM α -BAP by *E. coli/Sygdh-Sys1* in the *n*-hexane/buffer (6:4, v/v) biphasic system was monitored by chiral GC. After reaction for 6 h, (S)-BPE was obtained with over 99.9% *ee* and 98.3% yield (Fig. 7c, d). In this reaction, the TTN of NADP⁺ was 200 mol/mol, which was mainly limited by the low productivity of SyS1 towards α -BAP. The higher TTN will be obtained if SyGDH is coupled with other excellent NAD(P)H-dependent dehydrogenases.

4. Conclusion

In summary, a codon-optimized gene (*Sygdh*) was synthesized based on the putative GDH gene of Ta0897 in *T. acidophilum* genome and expressed in *E. coli* BL21 (DE3). The enzymatic properties of SyGDH showed that it displayed a mild optimum temperature, high thermostability, wide pH tolerance and dual coenzyme dependency. Notably, SyGDH was resistant to various organic solvents. These excellent properties of SyGDH made it an attractive candidate for NAD(P)H regeneration, especially in an organic solvent reaction system. Furthermore, as an effective, environmental-friendly, and easy-to-handle biocatalyst, whole cells of *E. coli/Sygdh-Sys1* were applied to the asymmetric reduction of *m*-CPC in a DMSO/buffer system and α -BAP in an *n*-hexane/buffer biphasic system with the consumption of only 0.2 mM NADP⁺ and low-cost D-glucose, producing (R)-CCE and (S)-BPE with high *ee*_p and yield.

Declaration of Competing Interest

The authors declare that they have no known competing financial interests or personal relationships that could have appeared to influence the work reported in this paper.

Acknowledgments

This work was financially supported by the National Natural Science Foundation of China (No. 21676117), the National First-Class Discipline Program of Food Science and Technology of China (No.

JUFSTR20180101), the Natural Science Foundation of Jiangsu Province for Youth of China (No. BK20180622), and China Postdoctoral Science Foundation (No. 2018M630522). We are also grateful to Prof. Xianzhang Wu (School of Biotechnology, Jiangnan University) for providing technical assistance.

Appendix A. Supplementary data

Supplementary material related to this article can be found, in the online version, at doi:<https://doi.org/10.1016/j.procbio.2019.09.037>.

References

- [1] S. Kara, J.H. Schrittwieser, F. Hollmann, M.B. Ansorge-Schumacher, Recent trends and novel concepts in cofactor-dependent biotransformations, *Appl. Microbiol. Biotechnol.* 98 (2014) 1517–1529.
- [2] X.R. Wu, X.D. Gou, Y.J. Chen, Enzymatic preparation of *t*-butyl-6-cyano-(3R, 5R)-dihydroxyhexanoate by a whole-cell biocatalyst co-expressing carbonyl reductase and glucose dehydrogenase, *Process Biochem.* 50 (2015) 104–110.
- [3] X.T. Zhou, R.Z. Zhang, Y. Xu, H.B. Liang, J.W. Jiang, R. Xiao, Coupled (R)-carbonyl reductase and glucose dehydrogenase catalyzes (R)-1-phenyl-1,2-ethanediol biosynthesis with excellent stereochemical selectivity, *Process Biochem.* 50 (2015) 1807–1813.
- [4] S.W. Xia, H. Lin, Y.Z. Chen, Preparation of (R)-2-chloro-1-(*m*-chlorophenyl)ethanol by Lipzyme TL IM-catalyzed second resolution, *Chin. Chem. Lett.* 23 (2012) 289–292.
- [5] L.C. Rocha, H.V. Ferreira, E.F. Pimenta, R.G. Berlinck, M.O. Rezende, M.D. Landgraf, M.H. Selegim, L.D. Sette, A.L. Porto, Biotransformation of alpha-bromoacetophenones by the marine fungus *Aspergillus sydowii*, *Mar. Biotechnol.* 12 (2010) 552–557.
- [6] A. Weckbecker, H. Groger, W. Hummel, Regeneration of nicotinamide coenzymes: principles and applications for the synthesis of chiral compounds, *Adv. Biochem. Eng. Biotechnol.* 120 (2010) 195–242.
- [7] H.C. Lo, R.H. Fish, Biomimetic NAD(+) models for tandem cofactor regeneration, horse liver alcohol dehydrogenase recognition of 1,4-NADH derivatives, and chiral synthesis, *Angew. Chemie Int. Ed. English* 41 (2002) 478–481.
- [8] L. Josa-Cullere, A.S.K. Landenpera, A. Ribaucourt, G.T. Hofler, S. Gargiulo, Y.Y. Liu, J.H. Xu, J. Cassidy, F. Paradisi, D.J. Opperman, F. Hollmann, C.E. Paul, Synthetic biomimetic coenzymes and alcohol dehydrogenases for asymmetric catalysis, *Catalysts*. 9 (2019) 207–218.
- [9] Y.H. Song, M.X. Liu, L.P. Xie, C. You, J.S. Sun, Y.H.P.J. Zhang, A recombinant 12-His tagged *Pyrococcus furiosus* soluble [NiFe]-hydrogenase I overexpressed in *Thermococcus kodakarensis* KOD1 facilitates hydrogen-powered in vitro NADH regeneration, *Biotechnol. J.* 14 (2019) 1800301.
- [10] W. Shen, Y. Chen, S. Qiu, D.N. Wang, Y.J. Wang, Y.G. Zheng, Semi-rational engineering of a *Kluyveromyces lactis* aldo-keto reductase *KIAKR* for improved catalytic efficiency towards *t*-butyl 6-cyano-(3R, 5R)-dihydroxyhexanoate, *Enzyme Microb. Tech.* 132 (2020) 109413.
- [11] K.A. Lampel, B. Uratani, G.R. Chaudhry, R.F. Ramaley, S. Rudikoff, Characterization of the developmentally regulated *Bacillus subtilis* glucose dehydrogenase gene, *J. Bacteriol.* 166 (1986) 238–243.
- [12] T. Mitamura, I. Urabe, H. Okada, Enzymatic properties of isozymes and variants of glucose dehydrogenase from *Bacillus megaterium*, *Eur. J. Biochem.* 186 (1989) 389–393.
- [13] X.Y. Wu, H.T. Ding, L.P. Ke, Y.Y. Xin, X.F. Cheng, Characterization of an acid-resistant glucose 1-dehydrogenase from *Bacillus cereus* var. *mycoides*, *Rom. Biotech. Lett.* 17 (2012) 7540–7548.
- [14] T. Pongtharangkul, P. Chuekitumchorn, N. Suwanampa, P. Payongsri, K. Honda, W. Panbangred, Kinetic properties and stability of glucose dehydrogenase from *Bacillus amyloliquefaciens* SB5 and its potential for cofactor regeneration, *AMB Express* 5 (2015) 68–80.
- [15] E. Vazquez-Figueroa, J. Chaparro-Riggers, A.S. Bommarium, Development of a thermostable glucose dehydrogenase by a structure-guided consensus concept, *Chembiochem.* 8 (2007) 2295–2301.
- [16] T. Nagao, T. Mitamura, X.H. Wang, S. Negoro, T. Yomo, I. Urabe, H. Okada, Cloning, nucleotide sequences, and enzymatic properties of glucose dehydrogenase isozymes from *Bacillus megaterium* IAM1030, *J. Bacteriol.* 174 (1992) 5013–20.
- [17] Z.Q. Liu, S.C. Dong, H.H. Yin, Y.P. Xue, X.L. Tang, X.J. Zhang, J.Y. He, Y.G. Zheng, Enzymatic synthesis of an ezetimibe intermediate using carbonyl reductase coupled with glucose dehydrogenase in an aqueous-organic solvent system, *Bioresour. Technol. Rep.* 229 (2017) 26–32.
- [18] A. Ruepp, W. Graml, M.L. Santos-Martinez, K.K. Koretke, C. Volker, H.W. Mewes, D. Frishman, S. Stocker, A.N. Lupas, W. Baumeister, The genome sequence of the thermoacidophilic scavenger *Thermoplasma acidophilum*, *Nature* 407 (2000) 508–513.
- [19] Y. Nishiya, N. Tamura, T. Tamura, Analysis of bacterial glucose dehydrogenase homologs from thermoacidophilic archaeon *Thermoplasma acidophilum*: Finding and characterization of aldohexose dehydrogenase, *Biosci. Biotech. Biochem.* 68 (2004) 2451–2456.
- [20] Y. Yasutake, Y. Nishiya, N. Tamura, T. Tamura, Structural insights into unique substrate selectivity of *Thermoplasma acidophilum* D-aldohexose dehydrogenase, *J. Mol. Biol.* 367 (2007) 1034–1046.
- [21] L.D. Smith, N. Budgen, S.J. Bungard, M.J. Danson, D.W. Hough, Purification and characterization of glucose dehydrogenase from the thermoacidophilic archaeobacterium *Thermoplasma acidophilum*, *Biochem. J.* 261 (1989) 973–977.
- [22] J.R. Bright, D. Byrom, M.J. Danson, D.W. Hough, P. Towner, Cloning, sequencing and expression of the gene encoding glucose-dehydrogenase from the thermophilic archaeon *Thermoplasma acidophilum*, *Eur. J. Biochem.* 211 (1993) 549–554.
- [23] J. John, S.J. Crennell, D.W. Hough, M.J. Danson, G.L. Taylor, The Crystal structure of glucose dehydrogenase from *Thermoplasma acidophilum*, *Structure* 2 (1994) 385–393.
- [24] M.A.F. Delgove, D. Valencia, J. Sole, K.V. Bernaerts, S.M.A. De Wildeman, M. Guillen, G. Alvaro, High performing immobilized Baeyer-Villiger monooxygenase and glucose dehydrogenase for the synthesis of epsilon-caprolactone derivative, *Appl. Catal. A Gen.* 572 (2019) 134–141.
- [25] T. Yu, J.F. Li, L.J. Zhu, D. Hu, C. Deng, Y.T. Cai, M.C. Wu, Reduction of *m*-chlorophenacyl chloride coupled with regeneration of NADPH by recombinant *Escherichia coli* cells co-expressing both carbonyl reductase and glucose 1-dehydrogenase, *Ann. Microbiol.* 66 (2016) 343–350.
- [26] H.T. Ding, F. Gao, Y. Yu, B. Chen, Biochemical and computational insights on a novel acid-resistant and thermal-stable glucose 1-dehydrogenase, *Int. J. Mol. Sci.* 18 (2017) 1198–1214.
- [27] Y. Kanoh, S. Uehara, H. Iwata, K. Yoneda, T. Ohshima, H. Sakuraba, Structural insight into glucose dehydrogenase from the thermoacidophilic archaeon *Thermoplasma volcanium*, *Acta. Crystallogr. D.* 70 (2014) 1271–1280.
- [28] A. Waterhouse, M. Bertoni, S. Bienert, G. Studer, G. Tauriello, R. Gumienny, F.T. Heer, T.A.P. de Beer, C. Rempfer, L. Bordoli, R. Lepore, T. Schwede, SWISS-MODEL: homology modelling of protein structures and complexes, *Nucleic Acids Res.* 46 (2018) W296–W303.
- [29] H. Aiba, Y. Nishiya, M. Azuma, Y. Yokooji, H. Atomi, T. Imanaka, Characterization of a thermostable glucose dehydrogenase with strict substrate specificity from a hyperthermophilic archaeon *Thermoproteus* sp. GDH-1, *Biosci. Biotech. Biochem.* 79 (2015) 1094–1102.
- [30] B. Siebers, V.F. Wendisch, R. Hensel, Carbohydrate metabolism in *Thermoproteus tenax*: in vivo utilization of the non-phosphorylated Entner-Doudoroff pathway and characterization of its first enzyme, glucose dehydrogenase, *Arch. Microbiol.* 168 (1997) 120–127.
- [31] J. Li, R.Z. Zhang, Y. Xu, R. Xiao, K.P. Li, H.Y. Liu, J.W. Jiang, X.T. Zhou, L.H. Li, L.X. Zhou, Y. Gu, Ala258Phe substitution in *Bacillus* sp YX-1 glucose dehydrogenase improves its substrate preference for xylose, *Process Biochem.* 56 (2017) 124–131.
- [32] A. Angelov, O. Futterer, O. Valerius, G.H. Braus, W. Liebl, Properties of the recombinant glucose/galactose dehydrogenase from the extreme thermoacidophile, *Picrophilus torridus*, *FEBS J.* 272 (2005) 1054–1062.
- [33] P. Haferkamp, S. Kutschki, J. Treichel, H. Hemeda, K. Sewczyk, D. Hoffmann, M. Zaparty, B. Siebers, An additional glucose dehydrogenase from *Sulfolobus solfataricus*: fine-tuning of sugar degradation, *Biochem. Soc. Trans.* 39 (2011) 77–81.
- [34] C. Pire, J. Esclapez, J. Ferrer, M.J. Bonete, Heterologous overexpression of glucose dehydrogenase from the halophilic archaeon *Haloflex mediterranei*, an enzyme of the medium chain dehydrogenase/reductase family, *FEMS Microbiol. Lett.* 200 (2001) 221–227.
- [35] N. Boontim, K. Yoshimune, S. Lumyong, M. Moriguchi, Cloning of D-glucose dehydrogenase with a narrow substrate specificity from *Bacillus thuringiensis* M15, *Ann. Microbiol.* 56 (2006) 237–240.
- [36] H.T. Ding, Y.Q. Du, D.F. Liu, Z.L. Li, X.J. Chen, Y.H. Zhao, Cloning and expression in *E. coli* of an organic solvent-tolerant and alkali-resistant glucose 1-dehydrogenase from *Lysinibacillus sphaericus* G10, *Bioresour. Technol. Rep.* 102 (2011) 1528–1536.
- [37] H. Lin, Y.Z. Chen, X.Y. Xu, S.W. Xia, L.X. Wang, Preparation of key intermediates of adrenergic receptor agonists: Highly enantioselective production of (R)-alpha-halohydrins with *Saccharomyces cerevisiae* CGMCC 2.396, *J. Mol. Catal., B Enzym.* 57 (2009) 1–5.
- [38] Y. Ni, B.H. Zhang, Z.H. Sun, Efficient Synthesis of (R)-2-Chloro-1-(3-chlorophenyl) ethanol by permeabilized whole-cells of *Candida ontarioensis*, *Chinese J. Catal.* 33 (2012) 681–687.
- [39] D. Zhu, Y. Yang, L. Hua, Stereoselective enzymatic synthesis of chiral alcohols with the use of a carbonyl reductase from *Candida magnoliae* with anti-prelog enantioselectivity, *J. Org. Chem.* 71 (2006) 4202–4205.
- [40] J.Y. Zhou, Y. Wang, G.C. Xu, L. Wu, R.Z. Han, U. Schwaneberg, Y.J. Rao, Y.L. Zhao, J.H. Zhou, Y. Ni, Structural insight into enantioselective inversion of an alcohol dehydrogenase reveals a "Polar Gate" in stereorecognition of diaryl ketones, *J. Am. Chem. Soc.* 140 (2018) 12645–12654.
- [41] G.C. Xu, H.L. Yu, X.Y. Zhang, J.H. Xu, Access to optically active aryl halohydrins using a substrate-tolerant carbonyl reductase discovered from *Kluyveromyces thermotolerans*, *ACS Catal.* 2 (2012) 2566–2571.